Remarkable Stabilization of a Psychrotrophic RNase HI by a Combination of Thermostabilizing Mutations Identified by the Suppressor Mutation Method †

ARTICLE *in* BIOCHEMISTRY · AUGUST 2008

Impact Factor: 3.02 · DOI: 10.1021/bi800246e · Source: PubMed

7 AUTHORS, INCLUDING:

Takashi Tadokoro
National Institutes of Health
27 PUBLICATIONS **330** CITATIONS
SEE PROFILE

Muhammad Saifur Rohman
Gadjah Mada University
9 PUBLICATIONS **32** CITATIONS
SEE PROFILE

Yuichi Koga
Osaka University
91 PUBLICATIONS **969** CITATIONS
SEE PROFILE

Remarkable Stabilization of a Psychrotrophic RNase HI by a Combination of Thermostabilizing Mutations Identified by the Suppressor Mutation Method[†]

Takashi Tadokoro,[‡] Kyoko Matsushita,[‡] Yumi Abe,[‡] Muhammad Saifur Rohman,[‡] Yuichi Koga,[‡] Kazufumi Takano,[‡,§] and Shigenori Kanaya*[,‡]

Department of Material and Life Science, Graduate School of Engineering, Osaka University, 2-1 Yamadaoka, Suita, Osaka 565-0871, Japan, and CREST, JST, 2-1 Yamadaoka, Suita, Osaka 565-0871, Japan

Received February 12, 2008; Revised Manuscript Received May 16, 2008

ABSTRACT: Ribonuclease HI from the psychrotrophic bacterium *Shewanella oneidensis* MR-1 (So-RNase HI) is much less stable than *Escherichia coli* RNase HI (Ec-RNase HI) by 22.4 °C in T_m and 12.5 kJ mol^{-1} in $\Delta G(H_2O)$, despite their high degrees of structural and functional similarity. To examine whether the stability of So-RNase HI increases to a level similar to that of Ec-RNase HI via introduction of several mutations, the mutations that stabilize So-RNase HI were identified by the suppressor mutation method and combined. So-RNase HI and its variant with a C-terminal four-residue truncation (154-RNase HI) complemented the RNase H-dependent temperature-sensitive (ts) growth phenotype of *E. coli* strain MIC3001, while 153-RNase HI with a five-residue truncation could not. Analyses of the activity and stability of these truncated proteins suggest that 153-RNase HI is nonfunctional in vivo because of a great decrease in stability. Random mutagenesis of 153-RNase HI using error-prone PCR, followed by screening for the revertants, allowed us to identify six single suppressor mutations that make 153-RNase HI functional in vivo. Four of them markedly increased the stability of the wild-type protein by 3.6−6.7 °C in T_m and 1.7−5.2 kJ mol^{-1} in $\Delta G(H_2O)$. The effects of these mutations were nearly additive, and combination of these mutations increased protein stability by 18.7 °C in T_m and 12.2 kJ mol^{-1} in $\Delta G(H_2O)$. These results suggest that several residues are not optimal for the stability of So-RNase HI, and their replacement with other residues strikingly increases it to a level similar to that of the mesophilic counterpart.

Psychrophiles and psychrotrophs are defined as microorganisms that can grow even at around 0 °C (*1*). These microorganisms usually produce cold-adapted enzymes, which are characterized by increased activity at low temperatures and decreased stability as compared to those of their mesophilic counterparts (*2–5*). These enzymes share various structural features, such as a reduced number of ion pairs and hydrogen bonds, weakened hydrophobic interactions and packing at the core, an increased fraction of nonpolar surface area, a reduced surface hydrophilicity, a reduced helix stability, and a reduced number of the proline residues at the loop regions. However, the cold-adaptation mechanism of these enzymes remains to be fully understood. One of the promising strategies for understanding this mechanism is to construct the stabilized mutants of a given psychrophilic or psychrotrophic enzyme and analyze their stabilization mechanism. These studies enable us to identify conformational defects that make cold-adapted enzymes unstable. Directed evolution is a technique that mimics natural selection, enabling evolution and adaptation of enzymes under controlled conditions with well-defined pressures (*6–10*). The suppressor mutation method is similar to this technique (*11*). In this method, a mutant enzyme with decreased activity or stability is first constructed. Then, random mutagenesis is introduced into this mutant enzyme, and the resultant large mutant enzyme libraries are screened for the second-site revertants. Finally, the suppressor mutations identified in the second-site revertants are introduced into the wild-type enzyme. This method has been used to construct the *Escherichia coli* ribonuclease HI (Ec-RNase HI)[1] variants with increased stability (*12*) and *Thermus thermophilus* RNase HI (Tt-RNase HI) variants with enhanced activity (*13*). *E. coli* strain MIC3001 with *rnh*-339::cat and *rec*B270(Ts), which shows an RNase H-dependent temperature-sensitive (ts) growth phenotype (*14*), was used for these purposes. We used this method to construct the thermostabilized mutants of RNase HI from the psychrotrophic bacterium *Shewanella oneidensis* MR-1 (So-RNase HI).

RNase H (EC 3.1.26.4) is an enzyme that specifically cleaves the RNA strand of RNA−DNA hybrids (*15*). The enzyme is widely present in bacteria, archaea, eukaryotes, and retroviruses (*16*). These enzymes are involved in DNA

[†] This work was supported in part by a Grant-in-Aid for Scientific Research on Priority Areas "Systems Genomics" from the Ministry of Education, Culture, Sports, Science, and Technology of Japan and by the Industrial Technology Research Grant Program from the New Energy and Industrial Technology Development Organization (NEDO) of Japan.

* To whom correspondence should be addressed. Telephone and fax: +81-6-6879-7938. E-mail: kanaya@mls.eng.osaka-u.ac.jp.

[‡] Osaka University.

[§] CREST, JST.

[1] Abbreviations: RNase H, ribonuclease H; So-RNase HI, *Shewanella oneidensis* MR-1 RNase HI; Ec-RNase HI, *Escherichia coli* RNase HI; Tt-RNase HI, *Thermus thermophilus* RNase HI; CD, circular dichroism; GdnHCl, guanidine hydrochloride.

10.1021/bi800246e CCC: $40.75
Published on Web 07/11/2008

replication, repair, and transcription (*17–23*). So-RNase HI is a monomeric protein with 158 amino acid residues, and its amino acid sequence is 67% identical to that of its mesophilic counterpart, Ec-RNase HI, the structures and functions of which have been extensively studied (*24*). The crystal structure of So-RNase HI has been determined (*25*). This structure closely resembles that of Ec-RNase HI. Nevertheless, So-RNase HI is much less stable than Ec-RNase HI by 22.4 °C in T_m and 12.5 kJ mol^{-1} in $\Delta G(H_2O)$ (*25*). So-RNase HI is stabilized by 5.6 °C in T_m and 4.7 kJ mol^{-1} in $\Delta G(H_2O)$ by introducing an ion pair network into the region in which the C-terminal region of the βB strand interacts with βA, βC, and αV (*25*). This ion pair network is not present in So-RNase HI but is present in Ec-RNase HI. However, these values account for only one-third to one-fourth of the difference in stability between So-RNase HI and Ec-RNase HI.

Here we report that four of the six single mutations identified by the suppressor mutation method significantly increase the stability of So-RNase HI by 3.6−6.7 °C in T_m and 1.7−5.2 kJ mol^{-1} in $\Delta G(H_2O)$. Two other mutations also stabilize the protein, but only slightly. We also report that the effects of these mutations are additive, and simultaneous introduction of these four thermostabilizing mutations strikingly increase the stability of So-RNase HI by 18.7 °C in T_m and 12.2 kJ mol^{-1} in $\Delta G(H_2O)$. These values are comparable to those between So-RNase HI and Ec-RNase HI.

MATERIALS AND METHODS

Cells and Plasmid. E. coli MIC3001 [F^-, *supE44, supF58, lacY1 or* Δ*(lacIZY)6, trpR55, galK2, galT22, metB1, hsdR14*($r_K^- m_K^+$)*, rnhA339::cat, recB270*] (*14*) and *E. coli* MIC2067 [F^-,λ^-,IN(*rrn*D−*rrn*E)1,*rnhA339::cat, rnhB716::kam*] (*18*) were kindly donated by M. Itaya. λDE3 lysogens of these strains, *E. coli* MIC3001(DE3) and MIC2067(DE3), were previously constructed in our laboratory (*26*). Plasmid pET500M for overproduction of So-RNase HI was also previously constructed in our laboratory (*25*).

PCR. PCR was carried out with GeneAmp PCR system 2400 (GE Healthcare) using KOD polymerase (Toyobo), according to the procedure recommended by the supplier, except for error-prone PCR. Error-prone PCR was carried out using *Taq* DNA polymerase as described previously (*27, 28*) with slight modifications. It was carried out in the presence of 0.4−0.5 mM $MnCl_2$ to increase the error rate using GeneAmp PCR system 2400 at 94 °C for 30 s, 55 °C for 30 s, and 72 °C for 1 min for 30 cycles. The nucleotide sequences of the PCR products were determined or confirmed with a Prism 310 DNA sequencer (GE Healthcare). All oligonucleotides were synthesized by Hokkaido System Science.

Plasmid Construction. Plasmid pET500MC with a unique *Cla*I site was constructed by introducing this *Cla*I site into the 3′-terminal region of the So-RNase HI gene by changing the codon for Ile150 from ATA to ATC by PCR. The sequences of the PCR primers are 5′-AAGAAGGAGATATACATATGACTGAGCTCAAACT-3′ for the 5′-primer and 5′-GCGCGTCGACTTAAGACTCCGCCTGATAGCCAGT**ATCGAT**TTGCGTCGG-3′ for the 3′-primer, where underlined bases make up the *Nde*I (5′-primer) and *Sal*I (3′-primer) sites and boldface bases make up the *Cla*I site. Plasmid pET500M was used as a template. Plasmids pET500MC157, pET500MC156, pET500MC155, pET500MC154, and pET500MC153 were constructed by replacing the *Nde*I−*Sal*I fragment of pET500M containing the So-RNase HI gene with those containing the genes encoding 157-, 156-, 155-, 154-, and 153-RNase HI, respectively. These genes were amplified by PCR using the 5′-primer mentioned above and the 3′-primers designed such that a termination codon (TAA) is introduced into appropriate positions.

Random Mutagenesis and Screening. Random mutations were introduced into the 153-RNase HI gene by error-prone PCR using the primers used to amplify the 153-RNase HI gene. Plasmid pET500MC153 was used as a template. Amplified DNA fragments were digested with *Nde*I and *Sal*I and ligated with the large *Nde*I−*Sal*I fragment of pET500M in generating a library of the pET500MC153 derivatives.

The resultant library of the pET500MC153 derivatives was used to transform *E. coli* MIC3001(DE3) to screen for the revertants that restore the ability of 153-RNase HI to complement the ts growth phenotype of this strain. The transformants were spread on LB-agar plates with 50 mg/L ampicillin and 30 mg/L chroramphenicol, and these plates were incubated at both 30 and 42 °C. The colonies grown at 42 °C were selected as revertants, and the plasmid DNA was isolated from each clone. After confirming that each plasmid complements the ts growth phenotype of MIC3001(DE3), we determined the nucleotide sequences of the mutant 153-RNase HI genes.

The pET500MC derivatives for overproduction of the So-RNase HI derivatives with suppressor mutations were constructed by replacing the *Nde*I−*Cla*I fragment of pET500MC containing the So-RNase HI gene with those of the pET500MC153 derivatives containing suppressor mutations.

Site-Directed Mutagenesis. The genes encoding triple mutant protein N29R/D39A/M76V-RNase HI and quadruple mutant protein SM4-RNase HI were constructed by site-directed mutagenesis using PCR as described previously (*29*). Plasmid pET500M was used as a template. The mutagenic primers were designed such that the codons for Asn29 (AAT), Asp39 (GAT), Met76 (ATG), and Lys90 (AAA) are changed to those for Lys (AAG) or Arg (AGA), Gly (GGT) or Ala (GCT), Val (GTG), and Asn (AAT), respectively.

Overproduction and Purification. Overproduction and purification of all mutant proteins of So-RNase HI, except for 153-RNase HI, were carried out as described for the wild-type protein (*25*). 153-RNase HI was also purified as described for the wild-type protein, but in the presence of 10% glycerol. After purification, this mutant protein was dialyzed against 10 mM sodium acetate (pH 5.5) to remove glycerol. The protein concentration was determined from the UV absorption at 280 nm assuming that the absorption coefficient at this wavelength (2.1 for a 0.1% solution) is not changed by the mutation.

Enzymatic Activity. The RNase H activity was determined at 30 °C and pH 8.0 by measuring the radioactivity of the acid soluble digestion product from the ^{3}H-labeled M13 DNA−RNA hybrid, as described previously (*30*). The reaction mixture contained 10 pmol of the substrate and an appropriate amount of enzyme in 20 μL of 10 mM Tris-HCl (pH 8.0) containing 10 mM $MgCl_2$, 50 mM NaCl, 1 mM 2-mercaptoethanol, and 50 μg/mL BSA. One unit is

defined as the amount of enzyme producing 1 μmol of acid soluble material per minute. The specific activity was defined as the enzymatic activity per milligram of protein.

Circular Dichroism. The far-UV CD spectra were recorded on a J-725 spectropolarimeter (Japan Spectroscopic) at 4 °C. The protein was dissolved in 10 mM sodium acetate (pH 5.5). The protein concentration and optical path length were 0.1−0.2 mg/mL and 2 mm, respectively. The mean residue ellipticity, θ, which has units of degrees square centimeter per decimole, was calculated by using an average amino acid molecular weight of 110.

Thermal Denaturation. Thermal denaturation curves of So-RNase HI and its derivatives were measured as described previously (*25*). The proteins were dissolved in 10 mM sodium acetate (pH 5.5) or the same buffer containing 1 M GdnHCl. The protein concentration and optical path length were 0.1−0.2 mg/mL and 2 mm, respectively. The temperature of the protein solution was linearly increased by approximately 1.0 °C/min. Thermal denaturation of these proteins was not reversible in the absence of GdnHCl but was reversible in the presence of 1 M GdnHCl. The temperature of the midpoint of the transition, T_m, was calculated from curve fitting of the resultant CD values versus temperature data on the basis of a least-squares analysis. The enthalpy (ΔH_m) and entropy (ΔS_m) changes for thermal denaturation at T_m were calculated by van't Hoff analysis.

Urea-Induced Denaturation. Urea-induced denaturation curves of So-RNase HI and its derivatives were measured at 20 °C as described previously (*25*). The proteins (0.1−0.2 mg/mL) were dissolved in 10 mM sodium acetate (pH 5.5) containing 100 mM NaCl and the appropriate concentrations of urea. The protein solution was incubated for at least 2 h at 20 °C before the measurement. The urea-induced denaturation of these proteins was fully reversible. Assuming that the unfolding equilibria of these proteins follow a two-state mechanism, the pre- and post-transition baselines were extrapolated linearly, and the difference in free energy between the folded and unfolded states, ΔG, and the free energy change of unfolding in H_2O, $\Delta G(H_2O)$, were calculated by the equations given by Pace (*31*).

RESULTS

Stabilities and Activities of the So-RNase HI Derivatives with C-Terminal Truncations. To analyze the effect of the C-terminal truncation on the stability and activity of So-RNase HI, five mutant proteins, 157-, 156-, 155-, 154-, and 153-RNase HI, in which the one, two, three, four, and five C-terminal residues of So-RNase HI are truncated, respectively, were constructed. *E. coli* MIC3001(DE3) transformants with pET500M derivatives for overproduction of these mutant proteins were used to analyze whether they are functional in vivo. If the transformants for overproduction of a given mutant protein could grow at a nonpermissible temperature, 42 °C, we would judge that this mutant protein is functional in vivo. The transformants for overproduction of all mutant proteins, except for 153-RNase HI, could grow at 42 °C, suggesting that the C-terminal truncation of five residues or more is sufficient to make So-RNase HI nonfunctional in vivo.

Of the five mutant proteins, 153- and 154-RNase HI were overproduced in *E. coli* and purified to give a single band on sodium dodecyl sulfate−polyacrylamide gel electrophoresis (SDS−PAGE) (data not shown). The amount of protein purified from a 1 L culture was approximately 3 mg for 153-RNase HI and 5 mg for 154-RNase HI, both of which were considerably smaller than the amount of wild-type protein (~10 mg). This is mainly due to the low production levels of these mutant proteins as compared to that of the wild-type protein. The far-UV CD spectra of these mutant proteins were similar to that of the wild-type protein, suggesting that the main chain fold of the protein is not markedly changed by the truncation (data not shown). The specific activities of 153- and 154-RNase HI were 20 and 50%, respectively, of that of the wild-type protein (Table 1).

Stabilities of 153- and 154-RNase HI against thermal denaturation were analyzed by monitoring the change in the CD value at 220 nm. The thermal denaturation curves of these mutant proteins measured at pH 5.5 in the absence of GdnHCl indicate that the thermal stabilities of the wild-type protein, 154-RNase HI, and 153-RNase HI decrease in this order (Figure 1). Since thermal denaturation of these mutant proteins was not reversible under any condition that was examined, the thermodynamic parameters for unfolding of these mutant proteins could not be determined. However, the thermal denaturation curves of these mutant proteins were reproducible, unless the experimental condition was seriously changed. It is noted that So-RNase HI unfolds reversibly at pH 5.5 in the presence of 1 M GdnHCl (*25*). However, 154- and 153-RNase HI are not fully stable even at low temperatures in the presence of 1 M GdnHCl. From the thermal denaturation curves shown in Figure 1, the apparent T_m values, T_m(app), were determined to be 41.7 °C for 153-RNase HI and 44.4 °C for 154-RNase HI, which were lower than that of the wild-type protein by 10.0 and 7.3 °C, respectively (Table 1). These results indicate that destabilization by 7.3 °C in T_m is not enough to make So-RNase HI nonfunctional in vivo, but a further decrease in stability by 2.7 °C in T_m makes it nonfunctional in vivo. We used the gene encoding 153-RNase HI to screen for the revertants with amino acid substitutions that restore the stability of this mutant protein.

Identification of the Suppressor Mutations. When *E. coli* MIC3001(DE3) transformants with plasmid pET500M derivatives, in which random point mutations were introduced within the 153-RNase HI gene by the error-prone PCR methods, were examined for growth, approximately 0.5% of the colonies grew at 42 °C. Plasmid DNAs were isolated from 50 colonies grown at 42 °C and determined for the DNA sequences of the mutant 153-RNase HI genes. As a result, nine different genes encoding the 153-RNase HI derivatives, M1−M9, were obtained. The frequencies of these genes vary from 1 to 26. The suppressor mutations identified in these 153-RNase HI derivatives are summarized in Table 2. Of the nine 153-RNase HI derivatives, six (M1−M6) contain single mutations, two (M7 and M8) contain double mutations, and one (M9) contains tetra mutations.

Stabilities and Activities of the So-RNase HI Derivatives with Suppressor Mutations. To examine whether the suppressor mutations identified in the revertant mutants of 153-RNase HI increase the stability of the wild-type protein, six mutant proteins of So-RNase HI with single suppressor mutations identified in M1−M6 were constructed. They are

Table 1: Activities and Stabilities of So-RNase HI and Its Derivatives

protein	specific activity[a] (units/mg)	relative activity[a] (%)	T_m(app)[b] (°C)	ΔT_m(app)[b] (°C)	T_m[c] (°C)	ΔT_m[c] (°C)	$\Delta\Delta G_m$[c] (kJ mol^{-1})	ΔH_m[c] (kJ mol^{-1})
So-RNase HI	7.8	100	51.7	−	30.4	−	−	217
154-RNase HI	3.9	50	44.4	−7.3				
153-RNase HI	1.6	20	41.7	−10.0				
N29K-RNase HI	6.2	79			34.0	3.6	2.6	231
D39G-RNase HI	6.5	83			36.2	5.8	4.2	244
M76V-RNase HI	6.9	89			37.1	6.7	4.8	257
M81T-RNase HI	7.3	94			30.7	0.3	0.2	225
K90N-RNase HI	7.1	91			34.5	4.1	3.0	252
K124N-RNase HI	6.1	78			31.5	1.1	0.8	246
SM4-RNase HI	5.5	70			49.1	18.7	13.5	359
N29R/D39A/M76V-RNase HI	6.2	79			44.8	14.4	10.4	332
Ec-RNase HI[d]	9.1	120			52.8	22.4		325

[a] The enzymatic activity was determined at 30 °C using an M13 DNA−RNA hybrid as described in Materials and Methods. Each experiment was carried out at least twice, and the average value is shown. Errors are within 20% of the reported values. [b] Thermal denaturation curves of So-RNase HI and its truncated mutant proteins were measured at pH 5.5 in the absence of GdnHCl. Thermal denaturation of these proteins was not reversible under this condition. The apparent melting temperature, T_m(app), is the temperature of the midpoint of the thermal denaturation transition. The difference in the apparent melting temperature between the wild-type and mutant proteins, ΔT_m(app), is calculated as T_m(app)(mutant) − T_m(app)(wild-type). [c] Parameters characterizing the thermal denaturation of So-RNase HI and its derivatives. Thermal denaturation curves of these proteins were measured at pH 5.5 in the presence of 1 M GdnHCl. Thermal denaturation of these proteins, except for 154- and 153-RNase HI, was reversible under this condition. The melting temperature (T_m) is the temperature of the midpoint of the thermal denaturation transition. The difference in the melting temperature between the wild-type and mutant proteins (ΔT_m) is calculated as T_m(mutant) − T_m(wild-type). ΔH_m is the enthalpy change of unfolding at T_m calculated by van't Hoff analysis. The difference between the free energy change of unfolding of the mutant protein and that of the wild-type protein at T_m of the wild-type protein ($\Delta\Delta G_m$) was estimated by the equation $\Delta\Delta G_m = \Delta T_m \Delta S_m$(wild-type), where ΔS_m(wild-type) is the entropy change of the wild-type protein at T_m (*42*). The ΔS_m(wild-type) value of 0.72 kJ mol^{-1}, which was previously determined (*25*), was used to calculate the $\Delta\Delta G_m$ values. Errors are within ±0.3 °C for T_m, ±26 kJ mol^{-1} for ΔH_m, ±0.12 kJ mol^{-1} K for ΔS_m, and ±0.3 kJ mol^{-1} for $\Delta\Delta G_m$. [d] Data from ref *25*.

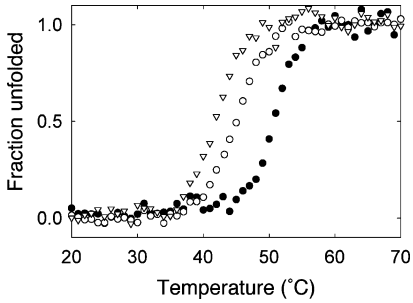

FIGURE 1: Thermal denaturation curves of the So-RNase HI derivatives with C-terminal truncation. The thermal denaturation curves of So-RNase HI (●), 154-RNase HI (○), and 153-RNase HI (▽) were obtained at pH 5.5 in the absence of GdnHCl by monitoring the change in the CD value at 220 nm as described in Materials and Methods.

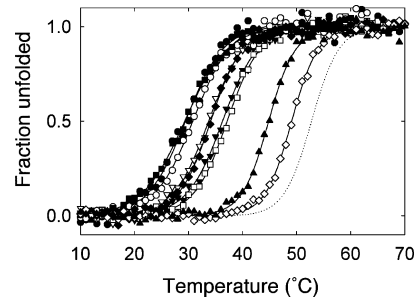

FIGURE 2: Thermal denaturation curves of the So-RNase HI derivatives with suppressor mutations. The thermal denaturation curves of So-RNase HI (●), N29K-RNase HI (▽), D39G-RNase HI (▼), M76V-RNase HI (□), M81T-RNase HI (○), K90N-RNase HI (◆), K124N-RNase HI (■), SM4-RNase HI (◇), and N29R/D39A/M76V-RNase HI (▲) were obtained at pH 5.5 in the presence of 1 M GdnHCl by monitoring the change in the CD value at 220 nm as described in Materials and Methods. The thermal denaturation curve of Ec-RNase HI (•••) is from ref *26*.

Table 2: 153-RNase HI Derivatives with Suppressor Mutations

protein	amino acid substitution	codon substitution	frequency
M1	Asn29 → Lys	AAT → AAG or AAA	26
M2	Asp39 → Gly	GAT → GGT	5
M3	Met76 → Val	ATG → GTG	8
M4	Met81 → Thr	ATG → ACG	2
M5	Lys90 → Asn	AAA → AAT	1
M6	Lys124 → Asn	AAA → AAG	3
M7	Lys35 → Arg	AAG → AGG	2
	Met81 → Thr	ATG → ACG	
M8	Lys111 → Glu	AAA → GAA	2
	Asp119 → Glu	GAT → GAA	
M9	Gly17 → Cys	GGC → CGC	1
	Ser71 → Ile	AGC → ATC	
	Lys90 → Arg	AAA → AGA	
	Val100 → Met	GTG → ATG	

N29K-, D39G-, M76V-, M81T-, K90N-, and K124N-RNase HI. All of the mutant proteins were overproduced in *E. coli* in a soluble form and purified to give a single band on SDS−PAGE (data not shown). The amounts of the mutant proteins purified from 1 L cultures were approximately 10 mg, which is similar to that of the wild-type protein. The far-UV CD spectra of all mutant proteins were similar to that of the wild-type protein (data not shown), suggesting that these mutations do not seriously affect the protein conformation. The specific activities of the mutant proteins are summarized in Table 1. They are similar to that of the wild-type protein, suggesting that none of the mutations seriously affects the enzymatic activity.

Stabilities of the mutant proteins against thermal denaturation were analyzed as described for 153- and 154-RNase HI, except that the thermal denaturation curves of these mutant proteins were measured at pH 5.5 in the presence of 1 M GdnHCl (Figure 2). Thermal denaturation of these mutant proteins was fully reversible under this condition. The thermodynamic parameters characterizing the thermal denaturation curves of the wild-type and mutant proteins are summarized in Table 1. The temperature of the midpoint of the transition, T_m, was 30.7−37.1 °C for mutant proteins and

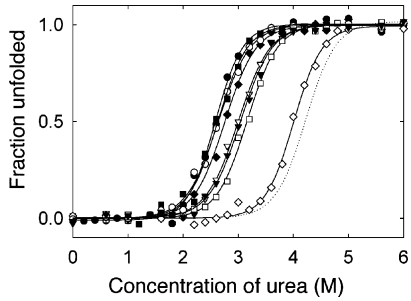

FIGURE 3: Urea-induced denaturation curves of the So-RNase HI derivatives with suppressor mutations. The urea-induced denaturation curves of So-, N29K-, D39G-, M76V-, M81T-, K90N-, K124N-, and SM4-RNase HI were obtained at pH 5.5 and 20 °C by monitoring the change in the CD value at 220 nm as described in Materials and Methods. The symbols for these proteins are the same as those shown in Figure 2. The urea-induced denaturation curve of Ec-RNase HI (•••) is from ref *25*.

Table 3: Parameters Characterizing Urea-Induced Denaturation of So-RNase HI and Its Derivatives[a]

protein	C_m (M)	m (kJ mol^{-1} M^{-1})	$\Delta G(H_2O)$ (kJ mol^{-1})	$\Delta\Delta G(H_2O)$ (kJ mol^{-1})
So-RNase HI	2.6	8.5	22.3	−
N29K-RNase HI	3.0	8.4	25.3	3.5
D39V-RNase HI	3.0	8.5	25.7	3.5
M76V-RNase HI	3.2	8.7	27.5	5.2
M81T-RNase HI	2.7	8.4	22.3	0.9
K90N-RNase HI	2.8	8.6	23.7	1.7
K124N-RNase HI	2.6	9.1	23.9	0
SM4-RNase HI	4.0	9.3	37.3	12.2
Ec-RNase HI[b]	4.3	8.2	34.8	12.5

[a] Urea-induced denaturation curves of these proteins were measured at pH 5.5 and 20 °C. Urea-induced denaturation of these proteins was reversible under this condition. The midpoint of the urea-induced denaturation curve (C_m), the measurement of the dependence of ΔG on the urea concentration (m), and the free energy change of unfolding in H_2O [$\Delta G(H_2O)$] were calculated from the urea-induced denaturation curves shown in Figure 4. The difference in $\Delta G(H_2O)$ [$\Delta\Delta G(H_2O)$] between the wild-type and mutant proteins was calculated by the equation $\Delta\Delta G(H_2O) = m_{av}\Delta C_m$, where m_{av} represents the average m value (8.7 kJ mol^{-1} M^{-1}) and $\Delta C_m = C_m$(mutant) − C_m(wild-type). Errors are within ±0.1 M for C_m, ±0.8 kJ mol^{-1} M^{-1} for m, and ±1.0 kJ mol^{-1} for $\Delta G(H_2O)$. [b] Data from ref *25*.

30.4 °C for the wild-type protein. Thus, all mutant proteins are more stable than the wild-type protein by 0.3−6.7 °C in T_m and 0.22−4.8 kJ mol^{-1} in ΔG_m.

Stabilities of the mutant proteins against urea-induced denaturation were also analyzed by monitoring the change in the CD values at 220 nm. The urea-induced denaturation curves of these proteins measured at pH 5.5 and 20 °C are shown in Figure 3. Urea-induced denaturation of these proteins was fully reversible under this condition and showed a two-state transition. The thermodynamic parameters characterizing the urea-induced denaturation curves of the wild-type and mutant proteins are summarized in Table 3. The apparent free energy changes of unfolding in the absence of denaturant, $\Delta G(H_2O)$, and midpoints of the denaturation curves, C_m, of all mutant proteins, except for K124N-RNase HI, were higher than those of the wild-type protein by 0.9−5.2 kJ mol^{-1} and 0.1−0.6 M, respectively. No significant difference was detected in these values between K124N-RNase HI and the wild-type protein. Thermal denaturation of this protein indicates that K124N-RNase HI is more stable than the wild-type protein, but by only 1.1 °C in T_m and 0.8 kJ mol^{-1} in ΔG_m. Thus, the stabilities of the mutant proteins against urea-induced denaturation show good agreement with those against thermal denaturation, although the $\Delta\Delta G(H_2O)$ and $\Delta\Delta G_m$ values are slightly different from each other for all mutant proteins.

Combination of the Thermostabilizing Mutations. To examine whether the effect of each thermostabilizing mutation is additive, the quadruple mutant protein of So-RNase HI with the Asn29 → Lys, Asp39 → Gly, Met76 → Val, and Lys90 → Asn mutations (SM4-RNase HI) was constructed. These four single mutations were chosen for construction of this quadruple mutant protein, because these mutations significantly increase the stability of So-RNase HI by 3.6−6.7 °C in T_m and 1.7−5.2 kJ mol^{-1} in $\Delta G(H_2O)$. SM4-RNase HI was overproduced in *E. coli* in a soluble form and purified to give a single band on SDS−PAGE (data not shown). The amount of protein purified from a 1 L culture was comparable to that of the wild-type protein. The far-UV CD spectrum of SM4-RNase HI was similar to that of the wild-type protein (data not shown), suggesting that these quadruple mutations do not seriously affect the protein conformation. The specific activity of SM4-RNase HI was 70% of that of the wild-type protein.

The stabilities of SM4-RNase HI against thermal denaturation (Figure 2) and urea-induced denaturation (Figure 3) were analyzed as mentioned above for the single mutant proteins. Thermal and urea-induced denaturation of SM4-RNase HI was fully reversible and showed a two-state transition. The thermodynamic parameters characterizing the thermal (Table 1) and urea-induced (Table 3) denaturation curves of SM4-RNase HI indicate that this quadruple mutant protein is more stable than the wild-type protein by 18.7 °C in T_m and 12.2 kJ mol^{-1} in $\Delta G(H_2O)$. These values are comparable to the sum of the ΔT_m (20.2 °C) and $\Delta\Delta G(H_2O)$ (13.9 kJ mol^{-1}) values of the four single mutations, indicating that the effects of the single mutations on protein stability are additive.

Stability of N39R/D39A/M76V-RNase HI. Of the four residues that are undoubtedly not optimal for the stability of So-RNase HI, Asn29, Asp39, and Met76 are replaced with Arg27, Ala37, and Val74 in Ec-RNase HI and Arg31, Gly41, and Leu78 in Tt-RNase HI, respectively. In contrast, Lys90 is conserved as Arg88 in Ec-RNase HI and Arg93 in Tt-RNase HI. Therefore, three of the four thermostabilizing mutations identified by the suppressor mutation method (Asn29 → Lys, Asp39 → Gly, and Met76 → Val) are the replacement of the residues of So-RNase HI with those of Ec-RNase HI or Tt-RNase HI. To measure how much the combination of these three changes can account for the stability difference between So-RNase HI and Ec-RNase HI, the triple mutant protein of So-RNase HI, N29R/D39A/M76V-RNase HI, was constructed. The production level and purification yield of this mutant protein were comparable to those of SM4-RNase HI. Its far-UV CD spectrum was similar to that of the wild-type protein (data not shown), suggesting that the triple mutations do not seriously affect the protein conformation. Its specific activity was 79% of that of the wild-type protein.

The stability of N29R/D39A/M76V-RNase HI against thermal denaturation was analyzed as mentioned above for the single mutant proteins (Figure 2). Thermal denaturation of this mutant protein was fully reversible and showed a two-state transition. The thermodynamic parameters character-

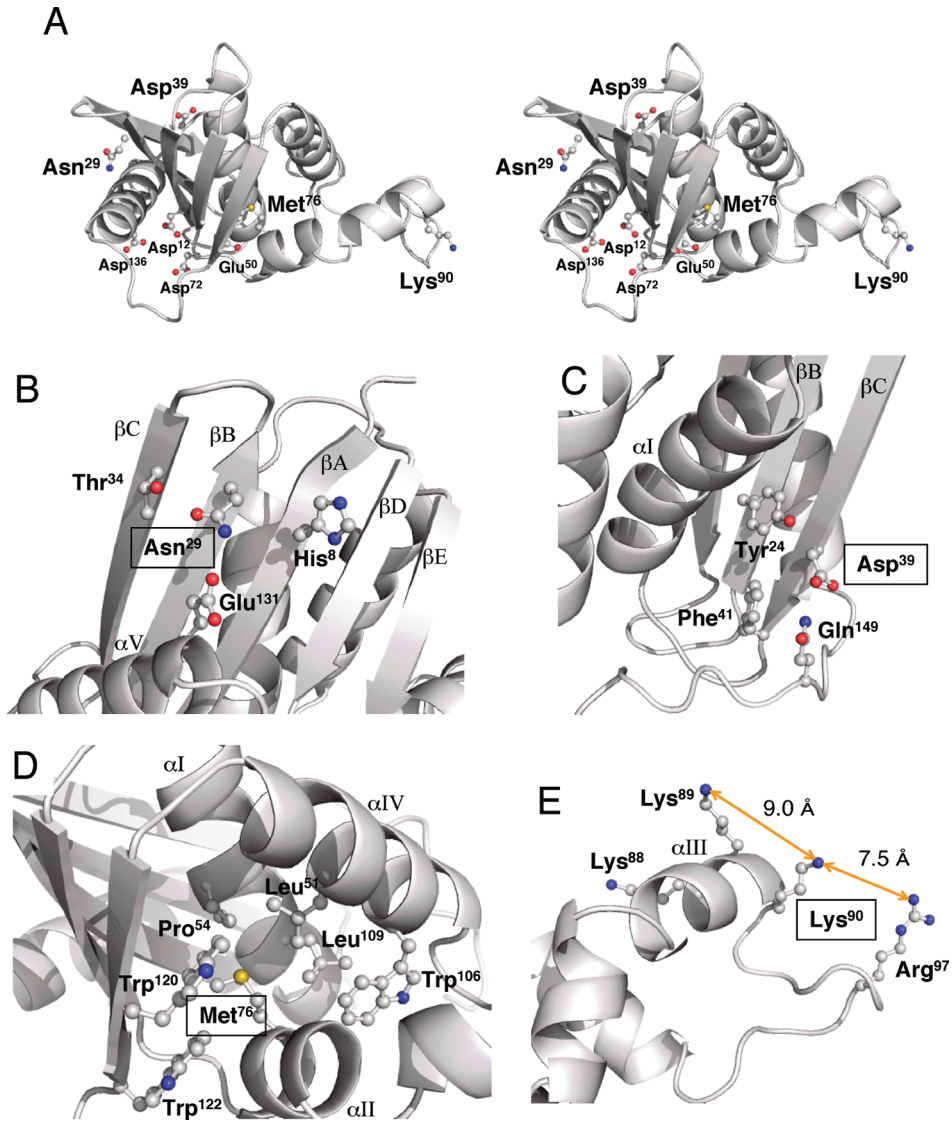

FIGURE 4: Crystal structure of So-RNase HI. (A) Stereoview of the entire backbone structure of So-RNase HI (PDB entry 2E4L). Four active site residues (Asp12, Glu50, Asp72, and Asp136), Asn29, Asp39, Met76, and Lys90 are shown as ball-and-stick models, in which the oxygen, nitrogen, and sulfur atoms are colored red, blue, and yellow, respectively. (B−E) Structures of the regions around Asn29 (B), Asp39 (C), Met76 (D), and Lys90 (E). These residues, as well as those which are located close to these residues, are shown as ball-and-stick models, in which the oxygen, nitrogen, and sulfur atoms are colored red, blue, and yellow, respectively. For panel E, possible positive charge repulsions between Lys90 and Lys89 and between Lys90 and Arg97 are shown by broken orange arrows together with their distances. All figures are generated using PyMOL (http://pymol.sourceforge.net/).

izing the thermal denaturation curve of this mutant protein are summarized in Table 1. N29R/D39A/M76V-RNase HI is more stable than the wild-type protein by 14.4 °C in T_m. This value is two-thirds of the difference in the T_m values between So-RNase HI and Ec-RNase HI (22.4 °C), indicating that the combination of the three changes accounts for two-thirds of the stability difference between So-RNase HI and Ec-RNase HI. The stability of N29R/D39A/M76V-RNase HI against urea-induced denaturation was not analyzed, because the stabilities of the single and quadruple mutant proteins against urea-induced denaturation show good agreement with those against thermal denaturation.

DISCUSSION

Additive Effects of Thermostabilizing Mutations. In this report, we showed that the suppressor mutation method is effective in identifying thermostabilizing mutations of psychrotrophic So-RNase HI and the combination of these thermostabilizing mutaitons is effective in strikingly stabilizing this protein. The resultant quadruple mutant protein is more stable than the wild-type protein by 18.7 °C in T_m and 12.2 kJ mol^{-1} in $\Delta G(H_2O)$. These differences are comparable to those between So-RNase HI and mesophilic Ec-RNase HI. Combination of the three mutations, which are designed to replace the residues of So-RNase HI with those of Ec-RNase HI, also increases the stability of So-RNase HI by 14.4 °C in T_m, which accounts for two-thirds of the difference in the T_m values between So-RNase HI and Ec-RNase HI. These results suggest that a psychrotrophic protein is destabilized as compared to its mesophilic counterpart by increasing the number of the residues that are not optimal for protein stability. It has been reported for other proteins that combination of multiple thermostabilizing mutations is quite effective in greatly increasing protein stability. For example, bacterial cold shock protein (*32*) and Gβ1 (*33*) are dramatically stabilized by 31.2 and 35.1 °C in T_m and 20.1

and 28.5 kJ mol^{-1} in ΔG, respectively, by the combination of the four stabilizing mutations. Likewise, Ec-RNase HI is stabilized by 20.2 °C in T_m and 23.4 kJ mol^{-1} in ΔG by the combination of the five stabilizing mutations (*34*), and T4 lysozyme is stabilized by 8.3 °C in T_m and 15.1 kJ mol^{-1} in ΔG by the combination of the seven stabilizing mutations (*35*). However, all of these proteins are mesophilic ones. Therefore, this is the first report of the remarkable stabilization of a psychrotrophic protein by the combination of multiple thermostabilizing mutations.

Possible Thermostabilization Mechanism by Mutation. According to the crystal structure of So-RNase HI, Asn29, Asp39, Met76, and Lys90 are distant from one another (Figure 4A). Because the replacement of Asn29, Asp39, and Met76 with the residues of Ec-RNase HI or Tt-RNase HI considerably increases the protein stability, these residues probably contribute to the destabilization of So-RNase HI as compared to Ec-RNase HI or Tt-RNase HI. Asn29 is not replaced with Arg, which is conserved in Ec-RNase HI and Tt-RNase HI, but is replaced with Lys. However, Lys is similar to Arg in both size and charge. In contrast, Lys90 may not contribute to it, because it is conserved as Arg in Ec-RNase HI and Tt-RNase HI. The stabilization mechanisms by the mutations of these residues, except for Asn29 → Arg and Asp39 → Ala, are discussed in more detail below. The stabilization mechanisms of the Asn29 → Arg and Asp39 → Ala mutations are not discussed, because the effects of these single mutations on the stability of So-RNase HI remain to be analyzed. However, the difference in the T_m values between So-RNase HI and N29R/D39A/M76V-RNase HI (14.4 °C) is comparable to the sum of the ΔT_m values of N29K-, D39G-, and M76V-RNase HI (16.1 °C) (Table 1), suggesting that the stabilization mechanisms of the Asn29 → Arg and Asp39 → Ala mutations are similar to those of the Asn29 → Lys and Asp39 → Gly mutations, respectively.

Asn29 → Lys. Asn29 is located in strand βB, which forms a β-sheet with four other β-strands (Figure 4B). In the vicinity of this residue are located His8, Thr34, and Glu131. Of these residues, only Glu131 is conserved as Glu129 in Ec-RNase HI. His8, Asn29, and Thr34 are replaced with Glu6, Arg27, and Glu32, respectively, in Ec-RNase HI. According to the crystal structure of Ec-RNase HI, Arg27 forms an ion pair network with Glu6, Glu32, and Glu131. Therefore, the Asn29 → Lys mutation stabilizes the protein, probably because an ion pair is newly formed between Lys29 and Glu131. We previously reported a similar result that the mutant protein of So-RNase HI, H8E/N29R/T34E-RNase HI, is more stable than the wild-type protein by 5.6 °C in T_m and 4.7 kJ mol^{-1} in $\Delta G(H_2O)$ (*25*). This triple mutant protein is designed to introduce an ion pair network in the region where Arg27 forms ion pairs with three glutamate residues. The difference in stability between N29K-RNase HI and So-RNase HI [3.6 °C in T_m and 3.5 kJ mol^{-1} in $\Delta G(H_2O)$] is smaller than that between H8E/N29R/T34E-RNase HI and So-RNase HI, probably because the number of ion pairs introduced by the single mutation is smaller than that introduced by the triple mutations.

Asp39 → Gly. Asp39 is located in strand βC (Figure 4C). In the vicinity of this residue are located Tyr24, Phe41, and Gln149. The distance between either one of these residues and Asp39 is <8 Å, suggesting that the side chain of Asp39 causes steric hindrance with these residues. Asp39 is replaced with Ala37 in Ec-RNase HI and Gly41 in Tt-RNase HI. Asp39 is partially buried inside the protein molecule, while Ala37 and Gly41 are almost fully buried inside the protein molecule. The Asp39 → Gly mutation stabilizes the protein, probably because a steric hindrance between Asp39 and surrounding residues is eliminated, and polar atoms are removed from a hydrophobic environment.

Met76 → Val. Met76 is located in helix αII, and its side chain is almost fully buried inside the protein molecule (Figure 4D). This residue is one of the constituents of the hydrophobic core, which is formed by Leu51, Pro54, Met76, Trp106, Leu109, Trp120, and Trp122. All of these residues, except Pro54 and Met76, are fully conserved in Ec-RNase HI. Pro54 and Met76 are replaced with Ala52 and Val74, respectively, in Ec-RNase HI. Therefore, the Met76 → Val mutation stabilizes the protein, probably because the packing and hydrophobic interactions of the core-forming residues are improved. Slight differences in the steric configurations of the conserved residues at the hydrophobic core between So- and Ec-RNase HI support this possibility. This methionine residue is conserved in another psychrotrophic RNase HI from *Shewanella* sp. SIB1, which is less stable than So-RNase HI and is overproduced in *E. coli* in an insoluble form (*36*). As expected, the mutation of this residue to Val increases both the solubility and stability of SIB1 RNase HI (T. Tadokoro, personal communication). In addition, we previously showed that the Val74 → Leu mutation (cavity-filling mutation) stabilizes Ec-RNase HI by reducing the volume of the cavity around this residue (*37*). Tt-RNase HI contains Leu78 at the same position. These results suggest that this position is important for regulating the protein stability by changing the packing and hydrophobic interactions of the core-forming residues.

It is noted that the Ala52 → Pro mutation destabilizes Ec-RNase HI by 5.4 °C in T_m (*38*). However, the reciprocal mutation (Pro54 → Ala) stabilizes So-RNase HI by only 1.2 °C in T_m (T. Tadokoro, personal communication).

Lys90 → Asn. Lys90 is located in the "basic protrusion", which is important for substrate binding (*39*) (Figure 4E). It has been reported that unfavorable charge−charge interactions at the molecular surface of Ec-RNase HI decrease the protein stability (*40*). Two positively charged residues, Lys89 and Arg97, are located relatively close to Asp90. The distances between the Nζ atoms of Lys90 and Lys89 and between the Nζ atom of Lys90 and the Nη2 atom of Arg97 are 9.0 and 7.5 Å, respectively. Therefore, the Lys90 → Asn mutation stabilizes the protein, probably because a positive charge repulsion among these residues is eliminated. Protein stabilization by elimination of long-range repulsive interactions among charged residues has also been reported for a cold shock protein (*41*).

REFERENCES

1. Morita, R. Y., and Moyer, C. L. (2000) Origin of psychrophiles. In *Encyclopedia of biodiversity* (Levin, S. A., Colwell, R., Dailey, G., Lubchenco, J., Mooney, H. A., Schulze, E. D., and Tilman, G. D., Eds.) Vol. 4, pp 917−924, Academic Press, San Diego.
2. Smalas, A. O., Leiros, H. K., Os, V., and Willassen, N. P. (2000) Cold adapted enzymes. *Biotechnol. Annu. Rev. 6*, 1–57.
3. Gianese, G., Bossa, F., and Pascarella, S. (2002) Comparative structural analysis of psychrophilic and meso- and thermophilic enzymes. *Proteins 47*, 236–249.
4. Feller, G., and Gerday, C. (2003) Psychrophilic enzymes: Hot topics in cold adaptation. *Nat. Rev. Microbiol. 1*, 200–208.

5. Siddiqui, K. S., and Cavicchioli, R. (2006) Cold-adapted enzymes. *Annu. Rev. Biochem. 75*, 403–433.
6. Arnold, F. H. (1996) Combinatorial and computational challenges for biocatalyst design. *Nature 409*, 253–257.
7. Arnold, F. H., Wintrode, P. L., Miyazaki, K., and Gershenson, A. (2001) How enzymes adapt: Lessons from directed evolution. *Trends Biochem. Sci. 26*, 100–106.
8. Farinas, E., Butler, T., and Arnold, F. (2001) Directed enzyme evolution. *Curr. Opin. Biotechnol. 12*, 545–551.
9. Yuan, L., Kurek, I., English, J., and Keenan, R. (2005) Laboratory-directed protein evolution. *Microbiol. Mol. Biol. Rev. 69*, 373–392.
10. Johannes, T. W., and Zhao, H. (2006) Directed evolution of enzymes and biosynthetic pathways. *Curr. Opin. Microbiol. 9*, 261–267.
11. Kanaya, S. (2003) Screening of enzyme variants for thermostability. In *Enzyme functionality: Design, Engineering and Screening* (Svendsen, A., Ed.) pp 491−506, Marcel Dekker, New York.
12. Haruki, M., Noguchi, E., Akasako, A., Oobatake, M., Itaya, M., and Kanaya, S. (1994) A novel strategy for stabilization of *Escherichia coli* ribonuclease HI involving a screen for an intragenic suppressor of carboxyl-terminal delitions. *J. Biol. Chem. 269*, 26904–26911.
13. Hirano, N., Haruki, M., Morikawa, M., and Kanaya, S. (2000) Enhancement of the enzymatic activity of ribonuclease HI from *Thermus thermophilus* HB8 with a suppressor mutation method. *Biochemistry 39*, 13285–13294.
14. Itaya, M., and Crouch, R. J. (1991) A combination of RNase H (*rnh*) and *recBCD* or *sbcB* mutations in *Escherichia coli* K12 adversely affects growth. *Mol. Gen. Genet. 227*, 424–432.
15. Crouch, R. J., and Dirksen, M. L. (1982) Ribonuclease H. In *Nuclease* (Linn, S. M., and Robert, R. J., Eds.) pp 211−241, Cold Spring Harbor Laboratory Press, Plainview, NY.
16. Ohtani, N., Haruki, M., Morikawa, M., and Kanaya, S. (1999) Molecular diversities of RNases H. *J. Biosci. Bioeng. 88*, 12–19.
17. Kogoma, T., and Foster, P. L. (1998) Physiological functions of *E. coli* RNase HI. In *Ribonucleases H* (Crouch, R. J., and Toulme, J. J., Eds.) pp 39−66, INSERM, Paris.
18. Itaya, M., Omori, A., Kanaya, S., Crouch, R. J., Tanaka, T., and Kondo, K. (1999) Isolation of RNase H genes that are essential for growth of *Bacillus subtilis* 168. *J. Bacteriol. 181*, 2118–2123.
19. Qiu, J., Qian, Y., Frank, P., Wintersberger, U., and Shen, B. (1999) *Saccharomyces cerevisiae* RNase H(35) functions in RNA primer removal during lagging-strand DNA synthesis, most efficiently in cooperation with Rad27 nuclease. *Mol. Cell. Biol. 19*, 8361–8371.
20. Arudchandran, A., Cerritelli, S., Narimatsu, S., Itaya, M., Shin, D. Y., Shimada, Y., and Crouch, R. J. (2000) The absence of ribonuclease H1 or H2 alters the sensitivity of *Saccharomyces cerevisiae* to hydroxyurea, caffeine and ethyl methanesulphonate: Implications for roles of RNases H in DNA replication and repair. *Genes Cells 5*, 789–802.
21. Haruki, M., Tsunaka, Y., Morikawa, M., and Kanaya, S. (2002) Cleavage of a DNA-RNA-DNA/DNA chimeric substrate containing a single ribonucleotide at the DNA-RNA junction with prokaryotic RNases HII. *FEBS Lett. 531*, 204–208.
22. Rydberg, B., and Game, J. (2002) Excision of misincorporated ribonucleotides in DNA by RNase H (type 2) and FEN-1 in cell-free extracts. *Proc. Natl. Acad. Sci. U.S.A. 99*, 16654–16659.
23. Cerritelli, S. M., Frolova, E. G., Feng, C., Grinberg, A., Love, P. E., and Crouch, R. J. (2003) Failure to produce mitochondrial DNA results in embryonic lethality in *Rnaseh1* null mice. *Mol. Cell 11*, 807–815.
24. Kanaya, S. (1998) Enzymatic activity and protein stability of *E. coli* ribonuclease HI. In *Ribonucleases H* (Crouch, R. J., and Toulme, J. J., Eds.) pp 1−38, INSERM, Paris.
25. Tadokoro, T., You, D.-J., Abe, Y., Chon, H., Matsumura, H., Koga, Y., Takano, K., and Kanaya, S. (2007) Structural, thermodynamic, and mutational analyses of a psychrotrophic RNase HI. *Biochemistry 46*, 7460–7468.
26. Ohtani, N., Haruki, M., Muroya, A., Morikawa, M., and Kanaya, S. (2000) Characterization of ribonuclease HII from *Escherichia coli* overproduced in a soluble form. *J. Biochem. 127*, 895–899.
27. Leung, D. W., Chen, E., and Goeddel, D. V. (1989) A method for random mutagenesis of a defined DNA segment using a modified polymerase chain reaction. *Technique 1*, 11–15.
28. Cirino, P. C., Mayer, K. M., and Umeno, D. (2003) Generating mutant libraries using error-prone PCR. *Methods Mol. Biol. 231*, 3–9.
29. Horton, R. M., Cai, Z. L., Ho, S. N., and Pease, L. R. (1990) Gene splicing by overlap extension: Tailor-made genes using the polymerase chain reaction. *BioTechniques 8*, 528–535.
30. Kanaya, S., Katsuda, C., Kimura, S., Nakai, T., Kitakuni, E., Nakamura, H., Katayanagi, K., Morikawa, K., and Ikehara, M. (1991) Stabilization of *Escherichia coli* ribonuclease H by introduction of an artificial disulfide bond. *J. Biol. Chem. 266*, 6038–6044.
31. Pace, C. N. (1990) Measuring and increasing protein stability. *Trends Biotechnol. 8*, 93–98.
32. Wunderlich, M., Martin, A., and Schmid, F. X. (2005) Stabilization of the cold shock protein CspB from *Bacillus subtilis* by evolutionary optimization of Coulombic interactions. *J. Mol. Biol. 347*, 1063–1076.
33. Wunderlich, M., and Schmid, F. X. (2006) *In vitro* evolution of a hyperstable Gβ1 variant. *J. Mol. Biol. 363*, 545–557.
34. Akasako, A., Haruki, M., Oobatake, M., and Kanaya, S. (1995) High resistance of *Escherichia coli* ribonuclease HI variant with quintuple thermostabilizing mutations to thermal denaturation, acid denaturation, and proteolytic degradation. *Biochemistry 34*, 8115–8122.
35. Zhang, X. J., Baase, W. A., Shoichet, B. K., Wilson, K. P., and Matthews, B. W. (1995) Enhancement of protein stability by the combination of point mutations in T4 lysozyme is additive. *Protein Eng. 8*, 1017–1022.
36. Ohtani, N., Haruki, M., Morikawa, M., and Kanaya, S. (2001) Heat labile ribonuclease HI from a psychrotrophic bacterium: Gene cloning, characterization and site-directed mutagenesis. *Protein Eng. 14*, 975–982.
37. Ishikawa, K., Nakamura, H., Morikawa, K., and Kanya, S. (1993) Stabilization of *Escherichia coli* ribonuclease HI by cavity-filling mutations within a hydrophobic core. *Biochemistry 32*, 6171–6178.
38. Akasako, A., Haruki, M., Oobatake, M., and Kanaya, S. (1997) Conformational stabilities of *Escherichia coli* RNase HI variants with a series of amino acid substitutions at a cavity within the hydrophobic core. *J. Biol. Chem. 272*, 18686–18693.
39. Kanaya, S., Katsuda-Nakai, C., and Ikehara, M. (1991) Importance of the positive charge cluster in *Escherichia coli* ribonuclease HI for the effective binding of the substrate. *J. Biol. Chem. 266*, 11621–11627.
40. You, D.-J., Fukuchi, S., Nishikawa, K., Koga, Y., Takano, K., and Kanaya, S. (2007) Protein thermostabilization requires a fine-tuned placement of surface-charged residues. *J. Biochem. 142*, 507–516.
41. Perl, D., Mueller, U., Heinemann, U., and Schmid, F. X. (2000) Two exposed amino acid residues confer thermostability on a cold shock protein. *Nat. Struct. Biol. 7*, 380–383.
42. Becktel, W. J., and Schellman, J. A. (1987) Protein stability curves. *Biopolymers 26*, 1859–1877.

BI800246E